Inelastic electron scattering to collective states of ^{118}Sn

R. J. Peterson, J. J. Kraushaar, M. R. Braunstein, and J. H. Mitchell*

Nuclear Physics Laboratory, Department of Physics, University of Colorado, Boulder, Colorado 80309

(Received 30 April 1990)

Elastic and inelastic electron scattering has been carried out on ^{118}Sn with q_{eff} ranging from 0.40 to 1.15 fm^{-1}. Form factors for the giant isovector dipole and isoscalar quadrupole peaks have been obtained and compared to collective model calculations, with methods closely parallel to those used to treat alpha particle and pion scattering to these same states. The charge responses determined by pion and electron scattering agree within uncertainties for the giant quadrupole peak.

I. INTRODUCTION

High-frequency isoscalar giant quadrupole resonances (GQR) containing large fractions of the possible sum-rule strength serve as important reservoirs of collective strength, influencing many properties of low-lying nuclear states [1]. The experimental features of these persistent peaks above the continuum have largely become familiar from inelastic alpha-particle scattering [2]. Inelastic pion scattering to these same states has revealed in the asymmetry between π^- and π^+ strengths an apparent systematic breakdown of the isoscalar nature of the response when analyzed by methods used for alpha scattering [3,4]. The strengths for the 2^+ peak at an excitation of $65A^{-1/3}$ MeV become increasingly neutronlike for heavier targets, when data are analyzed in an isoscalar collective model.

One interpretation of this observation suggests that the large neutron decay probability for the unbound but otherwise isoscalar giant quadrupole state enriches the outer reaches of the transition density with neutrons, enhancing the scattering of π^- over π^+, due to the strong absorption of these projectiles and to the π^- sensitivity to neutron components [5]. This also implies that alpha-particle scattering excites primarily the same neutron-rich surface [6] and is not probing the strictly isoscalar response. If such a bias exists, the large body of alpha-scattering data to the GQR requires a reinterpretation.

A reaction probe that is not strongly absorbed will give a fairer evaluation of the overall transition strength, unbiased by surface features. Inelastic electron scattering forms the most convenient probe of the distribution of the GQR transition density. Such studies have been carried out for a number of middle-mass target nuclei [7–10] but they often must contend with a large radiative background and the partially resolved isovector giant dipole resonance (GDR), not populated strongly by alphas and pions. There has not been a close consistency in the data analysis of these several probes, nor in the nuclear models used to interpret the results.

We report here a study of ^{118}Sn by electron scattering using a high-energy, high-resolution system. The high beam energies used provide a smoother background beneath the peaks examined, and enable the experiment to be carried out at small angles to diminish possible transverse contributions. The high resolution permits a study of the low-lying transitions to complement the GQR results and provides a test for any sharp structure in the GQR itself. Good statistical accuracy is achieved to provide good judgment for the background under the GQR peaks.

Our purpose is to compare the transition rates for low-lying collective and giant 2^+ states to sum rules and to the results of previous studies by alpha particles and pions in a consistent fashion in order to clarify the isospin response of these important modes. We treat the GQR as a coherent peak above whatever smooth background lies beneath it. This will not locate all the multipole strength, but only that within this specific collective feature. The same collective model commonly used for analysis of hadronic scattering will be applied to electron scattering in this work. These several probes are differently sensitive to the isospin and radial distribution features of the quadrupole strength; the present approach allows a valid comparison of the results. Just this question of the isospin response of the GQR prompted a theoretical study of ^{118}Sn[11], and comparisons of those results to experimental observations from several probes will be provided. The present results and those of Ref. [12] for coincident electron scattering on ^{116}Sn agree that the isoscalar quadrupole charge strength is less concentrated into a single peak than is indicated by open-shell random-phase-approximation (RPA) calculations.

II. EXPERIMENTAL METHODS

Electron beams of energies 147.4, 200.0, 225.0, and 356.0 MeV were provided by the MEA accelerator at NIKHEF-K in Amsterdam, with beam currents integrated by a toroid. Scattered electrons were analyzed in the high-resolution QDD spectrometer at a range of scattering angles from 29° to 56°. The ^{118}Sn scattering target was an isotopically enriched foil (15 mg/cm^2 enriched to 97.1%) mounted normal to the beam. Calibration of the scattered beam energies was made by scattering to the well-known levels of this target and to known levels in ^{64}Ni, ^{90}Zr, ^{12}C, and BeO. An overall resolution of 35 keV or better was achieved and excitation energies for sharp states were consistent to within 10 keV.

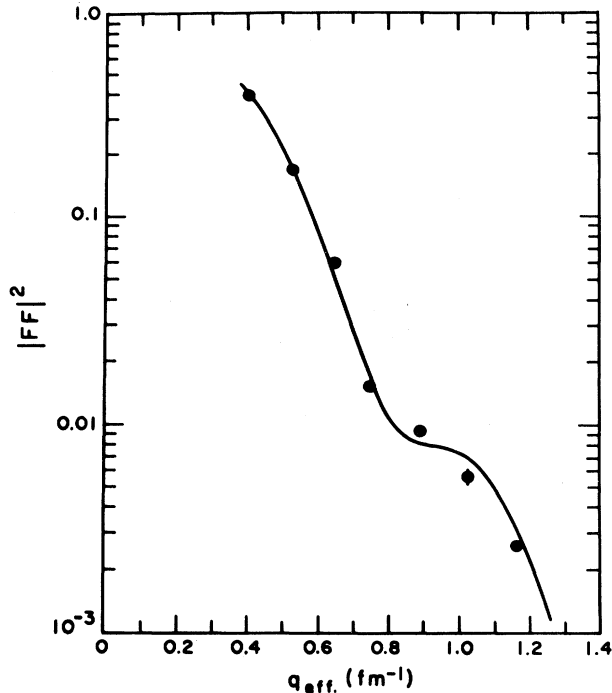Elastic-scattering cross sections for ^{118}Sn were deter-

FIG. 1. Elastic form factors for ^{118}Sn. The solid curve was calculated assuming a Gaussian charge distribution with the parameters of Ref. [13].

$q_{\rm eff}$ was carried out to check the normalization in a model-independent fashion. This adjustment was 1.01 ± 0.02 of cross sections to account for inaccuracies in target thickness, beam integration, and solid angle. Since the renormalization factor was unity to within the uncertainty, no correction was made.

The lowest-lying and sharp 2^+ and 3^- states were analyzed to compare to earlier measurements. Results for low-lying states of ^{64}Ni taken at the same time have been presented [14]. Figure 2 shows the low-lying region of ^{118}Sn with curves from the program ALLFIT [15] which include radiative tails and effects from the solid angle of the detector. The shape of the elastic peak was used for all sharp states in the spectra. The giant resonance spectrum is shown in Fig. 3.

Our goal is the characterization of the coherent enhancements of multipole strength occurring as a persistent feature above an unstructured background, with systematic excitation energies in all heavy nuclei. These are the giant resonances. The most severe problem besetting any inclusive giant resonance study is the estimation of the background beneath the broad peaks of interest. This background determination was aided, in an iterative way, by existing information on the giant peaks. Final results, as discussed below, differ somewhat from the initial parameters selected. We first constrained the position and full width at half maximum (FWHM) of the well-known isovector giant dipole resonance (GDR) to the values observed for photoabsorption data [16]. At low momentum transfers this is the dominant peak, and good fits were found when we drew a smooth background connecting the regions above and below the resonance and used a simple Gaussian peak shape. Although it has
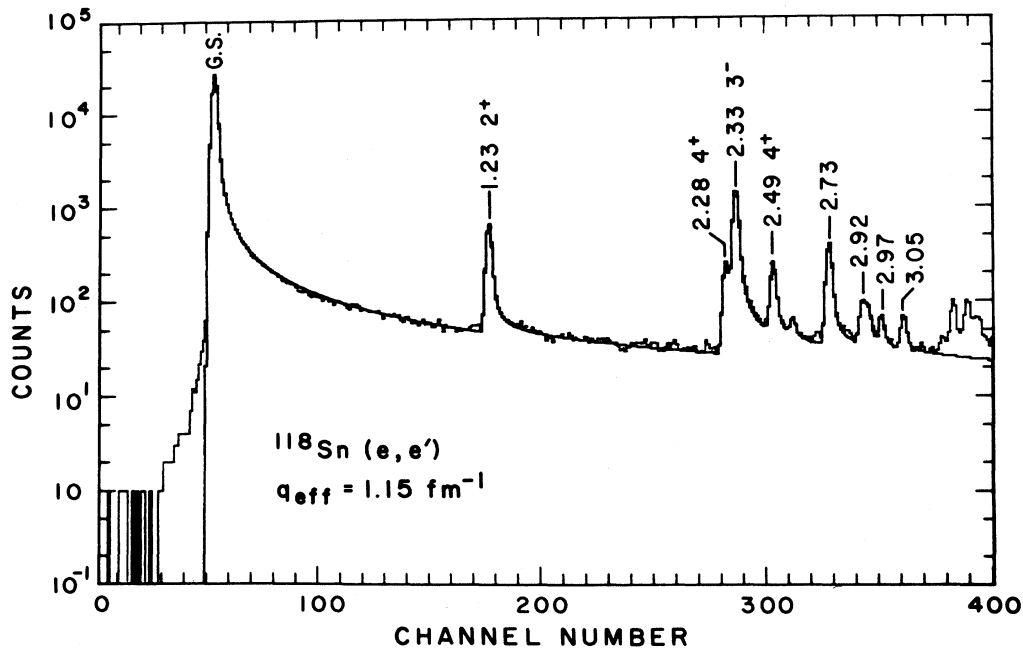
mined with results shown in Fig. 1. The curve is the result of calculations using a Gaussian charge distribution with parameters from Ref. [13]. A least-squares adjustment of the data using values at the lowest five values of

FIG. 2. Spectrum of low-lying states of ^{118}Sn with $q_{\rm eff}=1.5$ fm^{-1}. The solid line is a fit to the data which includes the radiative tails.
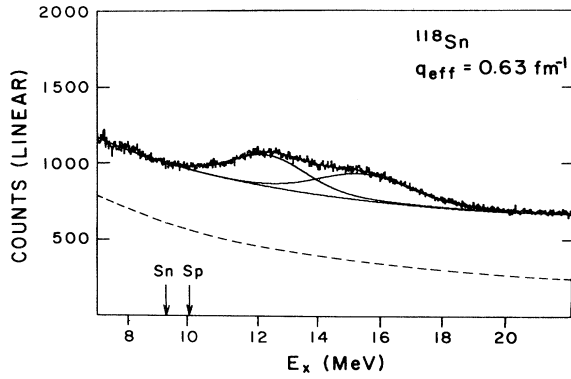
FIG. 3. Giant resonance region of the energy spectra for ^{118}Sn. The dashed line beneath the data is a continuation of the summed radiative tails from the elastic and strong inelastic states. The neutron and proton binding energies are shown. The background and fitting procedure are discussed in the text.

TABLE I. The geometrical parameters are listed for the charge distribution of ^{118}Sn used to evaluate radial matrix elements, to distort the projectile wave functions, and to form sum rules. The Fermi parameters are those of Ref. [13]. Only the isoscalar portion of the charge quadrupole sum rule, $\tilde{S}_z$, is listed.

Fermi parameters	
c (fm)	5.41
z (fm)	0.517
w	0
$\langle r^2 \rangle^{1/2}$ (fm)	4.634
$\tilde{S}_Z$ (e^2 fm^4 MeV)	3.756×10^4
D_Z (e^2 fm^2 MeV)	428.2

been concluded that the Gaussian shape is not appropriate for photoabsorption measurements [17], the difference is mainly in the tails of the peak. For spectra measured at a higher q, where the GQR is more visible, a similar background was drawn, as shown in Fig. 3. The GQR location was first fixed to be that observed in alpha scattering on ^{118}Sn [2] and the separation from the centroid of the GDR was fixed to the known value. This ensures that we are treating the same peak as seen in alpha and pion scattering and is the same as step I in Ref. [18]. Next, the position, width, and amplitude of the GQR and of the GDR were varied slightly, using Gaussian peak shapes, for a fit. This Gaussian shape for the GQR was used for consistency with the alpha and pion scattering work. The widths and centroids found for the best cases for each momentum transfer were averaged and a final fit to the area of each peak carried out using these values. This fit is seen in Fig. 3. Some spectra under duplicated conditions were independently fitted and yielded consistent results.

Two striking features were found. First, we observe no sharp structure in the GQR or GDR peaks with our 35 keV resolution. This is in contrast to the case of ^{208}Pb [19]. Second, the width of the peak at the standard GQR position in ^{118}Sn is somewhat narrower for electron scattering than seen in alpha scattering. For ^{118}Sn, the FWHM are 2.9 ± 0.4 MeV in the present work and 3.5 ± 0.3 MeV from Ref. [20]. Overall, the quality of the fits is very good. Backgrounds are found to be very similar in shape to those fit under the giant peaks in pion [3] scattering for this target. Uncertainties in the extracted form factors were estimated from the results of a range of fits, with different peak shapes and background curves.

Some of the assumed smooth background is due to the radiative tail of the elastic and low-lying peaks. For reference, the radiative tail from the elastic peak and strong low-lying inelastic states is shown in Fig. 3, where it is seen that approximately half of the background is due to this source. The rest of the continuum contains a wide rangle of multipoles, as shown in Ref. [9].

III. NUCLEAR REACTION MODELS

All measured form factors for $L \geq 2$ will be compared to form factors calculated using collective transition densities of the Tassie form [21] appropriate to giant states [22]:

$$\rho_{\mathrm{tr}}(r) \propto r^{L-1} \frac{d\rho(r)}{dr} .$$

The parameters for the ground-state charge distribution $\rho(r)$ are taken from previous results [13], with Woods-Saxon parameters listed in Table I. The same choices were used for the analysis of $(e, e'n)$ data for ^{116}Sn [12]. The Tassie form was also used for the pion scattering analysis [3], but the derivative form has been used for alpha-particle scattering [2,20]. If the Tassie form had been used, the alpha-particle strengths (isoscalar sum-rule fractions) would be less by a factor of about 0.75 for typical $L = 2$ cases.

Electron-scattering form factors were computed in the distorted-wave Born approximation (DWBA) [23] with a scale factor of the electric longitudinal reduced transition probability $B(CL)\uparrow$, and comparison to the data yields a single strength $B(CL)\uparrow$ for each observed transition. Summed over all transitions, these would form the energy-weighted sum rule:

$$S_Z = \sum_i (\hbar\omega_i) B(CL)\uparrow_i$$

$$= Z \frac{\hbar^2}{2M} \frac{e^2}{4\pi} L(2L+1)^2 \langle r^{2L-2} \rangle .$$

Since we will show results for the nominally isoscalar GQR, only a fraction Z/A of this strength is expected in this mode and we compare our data to [24]

$$\tilde{S}_Z = \sum_{i=\mathrm{IS}} \hbar\omega_i B(CL)\uparrow_i$$

$$= \frac{Z^2}{A} \frac{\hbar^2}{2M} \frac{e^2}{4\pi} L(2L+1)^2 \langle r^{2L-2} \rangle ,$$

as is standard for other electron-scattering results. The radial moment is evaluated for the ground-state charge distribution. This sum is listed in Table I.

In terms of these sum-rule (SR) strengths, the fraction exhausted by any transition at $\hbar\omega$ is given by

$$F_Z^{SR} = B(CL)\!\uparrow\!\hbar\omega/S_Z$$

or

$$\widetilde{F}_Z^{\,SR} = B(CL)\!\uparrow\!\hbar\omega/\widetilde{S}_Z$$

for the isoscalar GQR only.

Nuclear transition matrix elements are defined by

$$B(CL)\!\uparrow\; = e^2|M_p|^2 \quad \text{for change transitions}$$

and

$$B(0L)\!\uparrow\; = |M_0|^2 \quad \text{for isoscalar transitions.}$$

Inelastic pion scattering can also yield values for $|M_p|^2$ and $|M_0|^2$. Those results [3] will be compared to the present results for electron scattering for the low and giant collective states.

From inelastic alpha-particle scattering, an isoscalar strength may be inferred, but this can be related to the charge strength only through use of specific model. For a hydrodynamic oscillation, the neutron and proton matrix elements are in the ratio $M_n/M_p = N/Z$, and isoscalar matrix elements yield $M_0/M_p = A/Z$. The inferred charge reduced transition probability from alpha scattering is then

$$B^*(CL) = e^2(Z/A)^2 M_0^2 = e^2(Z/A)^2 B(0L)$$

and the sum-rule fractions for this inferred charge response are

$$F_Z^{*\,SR} = (Z/A)F_0^{SR}\;.$$

In the hydrodynamic model,

$$F_Z^{SR} = F_0^{SR}$$

to compare electromagnetic and isoscalar strengths. This is the relation implicitly used in Ref. [25], for instance, and shown in Ref. [24].

Three nuclear collective models were used to generate theoretical form factors to compare to the isovector GDR ($L=1$) data. We used the Goldhaber-Teller model of surface vibrations of neutron and proton matter [26]

$$\rho_{tr}^{GT} \propto \frac{d\rho}{dr}\;,$$

corresponding to the Tassie model for $L=1$, the Steinwedel-Jensen model of neutron and proton fluids oscillating within the smooth-edged volume [27]

$$\rho_{tr}^{SJ} \propto \rho(r)j_1\left[\frac{2.08r}{c}\right],$$

and the droplet model of Myers and Swiatecki [28]

$$\rho_{tr}^{MS} \propto \rho_{tr}^{GT} + \alpha\rho_{tr}^{SJ}\;.$$

The mixing parameter is $\alpha = 0.14216A^{1/3} = 0.697$ for ^{118}Sn. Calculated form factors, in DWBA, for all three models will be fitted to the GDR data to extract $B(C1)\!\uparrow$ values, which will be compared to the classical isovector GDR sum rule [29]

$$D_Z = \sum_{i=IV}\hbar\omega_i B(C1)\!\uparrow_i = \frac{NZ}{A}\frac{9}{4\pi}e^2\frac{\hbar^2}{2M}\;,$$

as listed in Table I.

Uncertainties for the $B(CL)$ factors are shown from the fitting or statistical uncertainties. This does not reflect the possible uncertainty in the theoretical form factors, which may be called the model dependence. Since the same transition densities are common to the pion and electron analyses for giant states, our use of the Tassie collective form is consistent, and is expected to be appropriate for the GQR on general theoretical grounds [22].

IV. LOW-LYING STATES OF ^{118}Sn

We treat here only the lowest 2^+ and 3^- transitions of ^{118}Sn to compare to previous work and for consistency with our giant resonance results. Since it is not our goal to provide accurate $B(CL)$ values for these well-know transitions, no extensive model-independent analysis will be presented.

Form factors for the first 2^+ and 3^- states of ^{118}Sn are shown in Fig. 4, compared to those computed with Tassie transition densities, as described above, by the solid curves. The best fits shown for the magnitudes give $B(C2)\!\uparrow\; = 1560\pm60\;e^2\,\text{fm}^4$ and $B(C3)\!\uparrow\; = (1.7\pm0.3)\times10^5\;e^2\,\text{fm}^6$. The lowest 2^+ state exhausts but 5% of the isoscalar charge sum-rule strength. In Table II these results are compared to previous electromagnetic results at lower momentum transfers. Our results for the 2_1^+ transition disagree beyond the stated statistical uncertainties with previous model-independent electron-scattering results at lower momentum transfer [30] and with Coulomb excitation [31]. Since we did not achieve accurate data at low momentum transfers for this transition, this disagreement is not surprising. For the 3_1^- transition, the good fit seen in Fig. 5 gives a value of $B(C3)\!\uparrow$ in very good agreement with the previous Tassie results [30]. If we use a phonon, not Tassie, nuclear model, smaller values of $B(CL)$ are obtained.

Proton matrix elements from pion scattering [3] square to give a $B(C3)\!\uparrow$ strength for ^{118}Sn in quite good agreement with the electromagnetic results, but the $B(C2)\!\uparrow$ obtained in this fashion is larger than the electromagnetic result. Isoscalar reduced transition probabilities should scale as $(Z/A)^2$ to match electromagnetic results in the hydrodynamic collective model. This is found to give agreement between alpha particle and pion scattering to the 2_1^+ and 3_1^- states. See Table II. These transition probabilities from hadron scattering are 30–40% greater than found by electromagnetic interactions. We point out these comparisons for the low-lying states in anticipation of a similar analysis for the giant states.

V. GIANT RESONANCES IN ^{118}Sn

A sample spectrum for the giant resonance region of ^{118}Sn is shown in Fig. 3. The fit shown was accomplished by constraining the separation of the two features to be

TABLE II. Results of the present work for ^{118}Sn are compared to previous electromagnetic, pion, and alpha-scattering results. Only statistical uncertainties are listed, save for the F^{SR} for the GQR, and Tassie (Goldhaber-Teller) models are used. The hydrodynamic model has been used to convert the pion and alpha results to the forms used here, with only the isoscalar portion of the charge sum rule for the GQR. Reduced electric transition probabilities are in e^2 fm^{2L}, with alpha-scattering results converted as in the text.

	$\frac{2^+}{B(C2)\uparrow}$	$\frac{3^-}{B(C3)\uparrow}$	$\frac{\text{GQR}}{B(C2)\uparrow}$	$\frac{\text{GQR}}{F_Z^{SR}}(\%)$
Present work	1560±60	(1.7±0.3)×10^5	770±40	25±5
(e,e')	2225^b	1.67±10^{5b}		32^a
CEX^c	1950			
$(\pi,\pi')^d$	3350	2.02×10^5	664	24±5
(α,α')	2830^e	2.22×10^{5e}	1970±420^e	70±15^e
	2250^f	1.39×10^{5f}	2307±700^f	84±25^f
$(e,e'n)^g$			1100±400	36±13

^{a}Reference [9], for ^{116}Sn. See text concerning the fitting procedures.
^{b}Tassie analysis, Ref. [30].
^{c}Reference [31].
^{d}Reference [3].
^{e}Reference [32], Tassie model for ^{120}Sn real geometry.
^{f}Reference [33] for ^{116}Sn.
^{g}Reference [12].

TABLE III. Results of the present experiment on ^{118}Sn are summarized for the lowest 2^+ and 3^- excitations, for the isoscalar GQR and for the isovector GDR peaks. The Tassie model is used for $L \geq 2$. For the isovector GDR, three models are used for reaction calculations to compare to the data, with differing magnitudes for $B(C1)$ and the fractions of the sum rule exhausted. The model of Goldhaber and Teller yields the most acceptable shape. Only the isoscalar portion of the charge sum rule was used for comparison to the $B(C2)$ values for the GQR only. Only statistical uncertainties are listed, and the systematic model dependence is not addressed in this table except for the sum-rule fraction for GQR. The energy weighting for the sum rule uses excitation energies from the present work.

	^{118}Sn
2^+	1.23 MeV
$B(C2)\uparrow$ $(e^2$ fm$^4)$	1560±60
3^-	2.32 MeV
$B(C3)\uparrow$ $(e^2$ fm$^6)$	(1.7±0.3)×10^5
GQR	12.35±0.2 MeV
Γ	2.9±0.4 MeV
$B(C2)\uparrow$ $(e^2$ fm$^4)$	770±40
F^{SR} (%)	25±5
GDR	15.55±0.2 MeV
Γ	3.7±0.4 MeV
Goldhaber-Teller	
$B(C1)\uparrow(e^2$ fm$^2)$	23±2
F^{SR} (%)	84±7
Steinwedel-Jensen	
$B(C1)\uparrow(e^2$ fm$^2)$	7.4±0.7
F^{SR} (%)	27±3
Myers-Swiatecki	
$B(C1)\uparrow(e^2$ fm$^2)$	13.7±1.3
F^{SR} (%)	50±5

3.2 MeV, determined by an average of fits to the better spectra, with fixed widths (FWHM) for the Gaussian peaks of 2.91 MeV (GQR) and 3.65 MeV (GDR). These shapes fit the data in Fig. 3 very well, with the empirical background shown. If the better spectra were fitted also allowing the widths to vary, the determinations indicate uncertainties in width of 0.4 MeV for both broad peaks. Centroids are at 12.35±0.2 MeV (GQR) and 15.55±0.2 MeV (GDR). The sum of the radiative tails from some of the elastic and sharp low-lying peaks is also shown.

Photoneutron studies of ^{118}Sn locate the GDR at 15.44 MeV with a Lorentzian FWHM of 4.86 MeV [16]. The Gaussian peak we locate agrees with this result in location, but is narrower. The form factor for the GDR is compared in Fig. 5 to those predicted, with good agreement in shape only for the Goldhaber-Teller (GT) model. This agrees with the results of Ref. [12], where this same GT model was used to remove GDR strength to present $C2/C0$ strength from the $(e,e'n)$ spectra on ^{116}Sn. The magnitude yields $B(C1)\uparrow=23\pm2$ e^2 fm^2, exhausting 84±7% of the sum-rule strength using the (GT) model. Results from other models are listed in Table III. The Steinwedel-Jensen (SJ) fit to the GDR data is poor, and yields but 27% of the sum-rule strength. The Myers-Swiatecki (MS) strength is more satisfactory, at 50%, but the fit is similar to the Steinwedel-Jensen fit. The strength from photoneutron studies is 1635 MeV− mb [16], or 114% of the sum-rule strength. These scattering and photonuclear measurements of the properties of the ^{118}Sn GDR thus agree reasonably well, confirming that this peak does contain essentially all the summed strength, representing a truly giant resonance.

With this success in the fitting to the electron-scattering spectra, we next analyze the GQR peak. An average location at 12.35±0.2 MeV was found, to be compared with 13.2 MeV found by alpha [2] scattering.

The recent $(e,e'n)$ study of ^{116}Sn found the GQR strength in a Lorentzian peak at 12.3±0.8 MeV, in concord with our observations [12]. The FWHM from the present work is 2.9±0.4 MeV, compared to 3.5±0.3 MeV from alpha scattering [2]. Fits to our electron spectra that insist upon use of these alpha-scattering results give an unacceptable deterioration of the results for the GDR peak.

Figure 5 shows the form factor for the feature at 12.35 MeV in ^{118}Sn, with a good fit to the computed Tassie form factor for $L=2$. The fit shown yields $B(C2)\uparrow=770\pm40$ e^2fm^4, which is but 25±1% of the strength expected for the isoscalar portion $\widetilde{S}_z$ of the classical sum given above. This uncertainty does not include

any systematic uncertainty due to a dependence upon the nuclear model used. Others [12] have estimated this to be a 20% effect, and we quote our sum-rule fraction to be 25±5%.

Our method of analysis removed the background by a smooth empirical curve. By demanding a coincidence with a decay neutron, the electron scattering of Ref. [12] also isolated a giant C2 peak in ^{116}Sn, with the same centroid as found in the present work. The strength is fitted to yield 36±13% of the sum rule, including an estimate of the model dependence.

Pion scattering studies [3] to the GQR matching the present usage yield a proton matrix element which squares to give $B(C2)\uparrow=664$ e^2fm^4, or 24±7% of the isoscalar portion $\widetilde{S}_z$ of the classical sum rule. This agrees very well with the present results. Inelastic alpha-particle scattering [2] to this same feature exhausts 65±15% of the isoscalar sum strength, which in the hydrodynamic model should agree with the present 25±5% result. We emphasize here the reminder that the analysis
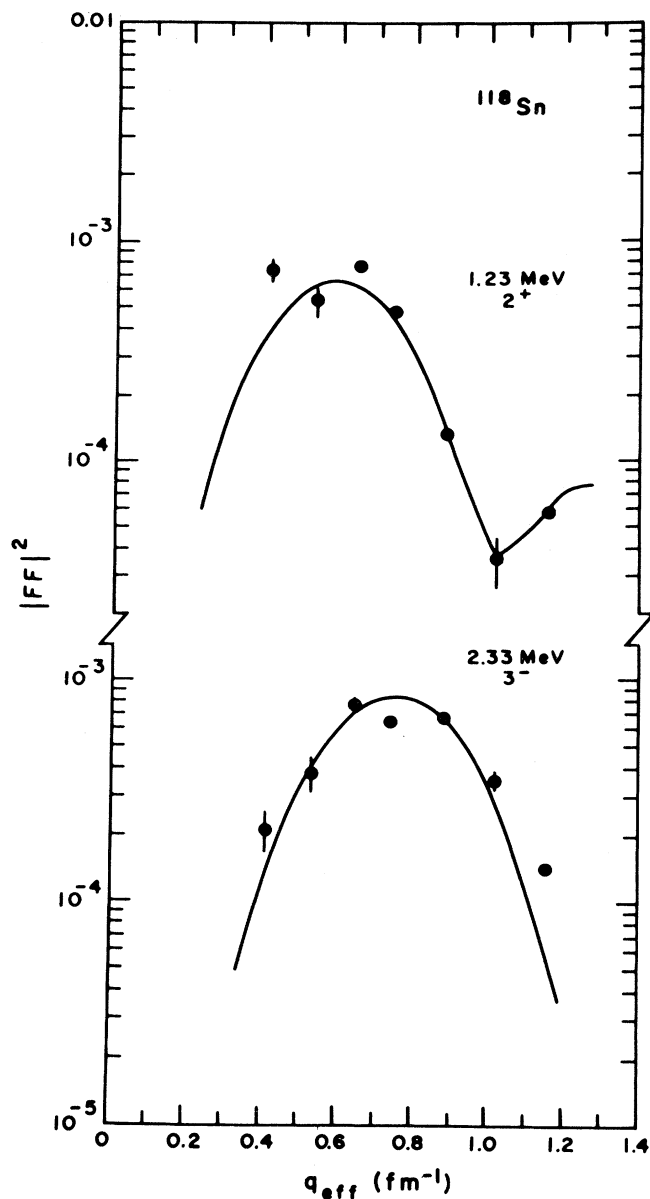

FIG. 4. Form factors for the lowest 2^+ and 3^- states in ^{118}Sn. The solid curves represent calculations carried out in DWBA with Tassie transition densities.
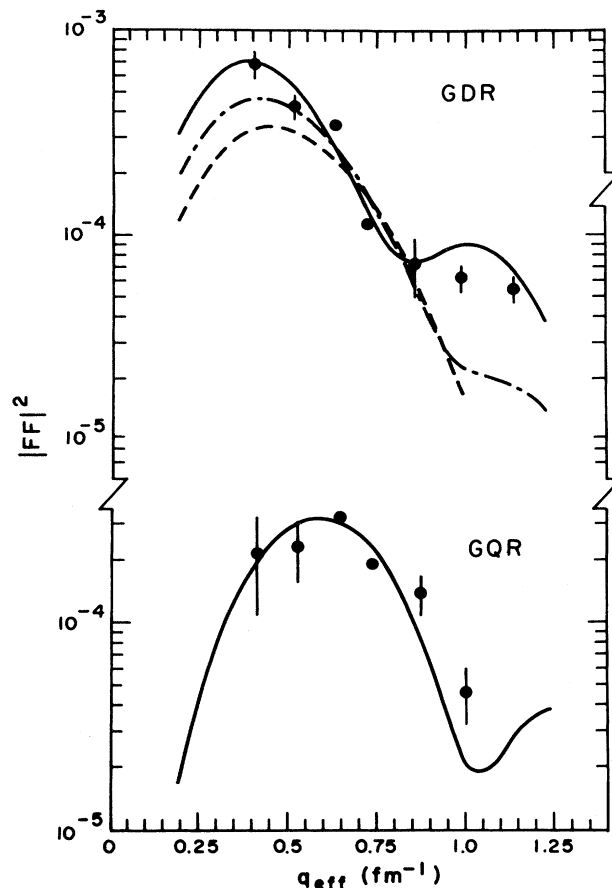

FIG. 5. Form factors for the giant resonances of ^{118}Sn. The solid curve for the GDR was calculated using the Goldhaber-Teller model to generate the form factors, the dashed curve uses the Steinwedel-Jensen model, and the dashed-dot curve uses the Myers-Swiatecki model. The curve shown for the GQR was calculated using a collective transition density of the Tassie form.

of the alpha-scattering data assumed the same transition density for neutron and proton components of the collective model, but was insensitive to this isospin composition. The analysis of π^+ and π^- data allows an explicit determination of the proton (Coulomb) strength.

The computed distribution of quadrupole strength in ^{118}Sn at high excitations is dominated by a peak at 13.2 MeV containing 100% of the isoscalar sum rule [11]. Electron-scattering data, originally shown as squares of form factors [9], were converted to a distribution of quadrupole strength in Fig. 5 of Ref. [11]. The electron data exhaust 65% of the isoscalar sum rule between 10 and 15 MeV, whereas the integral of the "data" shown in Ref. [11] is 4590 e^2 fm^4, or 158% of the sum rule. Evidently a factor of Z/A was misused in generating the curve for the electron data in Fig. 5 of Ref. [11]. Good agreement is found between the $C2$ strength in Ref. [9] itself and the present work.

We show in Fig. 6(a) the distribution of electron data of Ref. [9] as shown in Ref. [11], such that the integral concurs with the original results. Also shown in Fig. 6(a) are the present peak for the GQR and the peak from the pion data, averaged for the data at two beam energies [3,34] and using the methods of Ref. [3] to determine the proton strength. Numerical summaries of these data are listed in Table IV.

In the lower part of Fig. 6 are shown the data for the fitted peak in the present work compared to coincident data for ^{116}Sn($e,e'n$) from Ref. [12]. The theoretical distribution of strength (theory A) from Ref. [11] is shown for comparison. Harmonic-oscillator wave functions were used to obtain this result.

It is clear that the present inclusive electron data, the coincident electron data, the pion data, and the peak portion of the Tohuku electron data all agree in the distribution of the quadrupole strength. We have fitted the electron data of Ref. [9], with the background shown in Fig. 6, to extract results directly comparable to the other peak
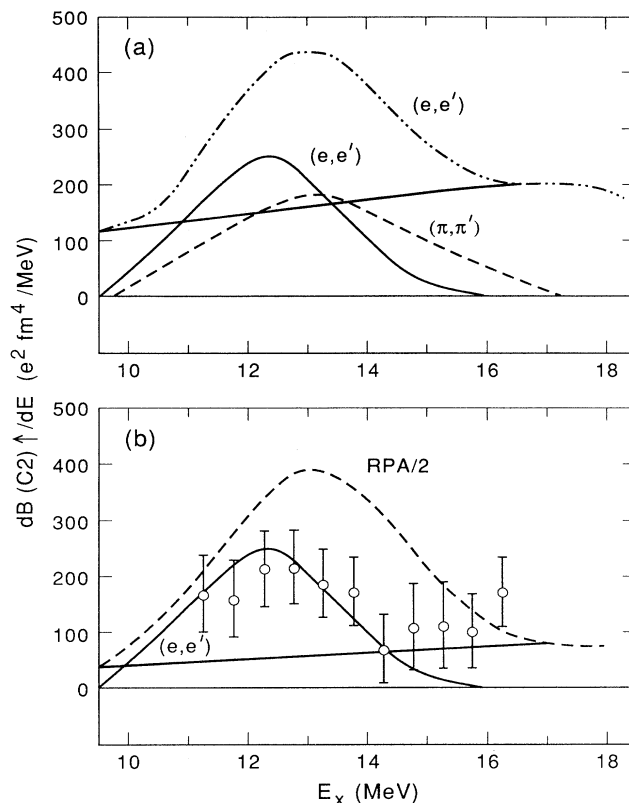

FIG. 6. (a) The GQR peaks as found in the present work (solid line) and in pion scattering (dashed line). They are compared to the distribution of quadrupole strength seen in electron scattering (Ref. [9]) by the dashed-dot-dot curve. The peak of this distribution was fitted using the linear background shown. (b) The present GQR peak compared to the data points found in the recent ($e,e'n$) experiment of ^{116}Sn (Ref. [12]). The dashed curve is the RPA calculation, scaled by 0.5, and the peak was fitted with the background shown. The numerical values of these peaks are in Table IV.

TABLE IV. Results of fitting a Gaussian peak shape to the GQR in ^{118}Sn, above a smooth background. The same methods were used for fitting electron, pion, and alpha-scattering data and RPA calculations. A single peak at 13.2 MeV exhausting 100% of the isoscalar portion of the quadrupole charge sum rule would have $B(C2)\uparrow = 2902$ e^2 fm^4. Uncertainties do not include any model dependence.

	Centroid (MeV)	Width FWHM(MeV)	$B(C2)\uparrow$ (e^2 fm^4)	Reference
RPA-A	13.2	(4)	2710	[11]
RPA-B	12.9	(4)	1070	[11]
^{116}Sn(e,e')	12.8	3.3	917	[9]
^{116}Sn($e,e'n$)	12.3±0.8		1100±400	[12]
(π,π')	13.2	3.8	664±66	[3,34]
(e,e')	12.4±0.2	2.9±0.4	770±40	present
(π,π') (via isoscalar)	13.2	3.8	1440±250	[3,34]
(α,α')(^{120}Sn)	13.3±03	3.7±0.5	1960±420	[32]
(^{120}Sn)	12.75±0.25	3.7±0.3	2190±450	[35]
(^{116}Sn)	13.2±0.2	3.3±0.2	2520±750	[33]
CEX	12.7	3.8	830	[39] fit by us

fitting methods. All four sources agree that the GQR peak contains about $800\ e^2\,\mathrm{fm}^4$, or 28% of the isoscalar sum rule, although the statistical accuracy of the $(e,e'n)$ data does not permit a distinction between continuum and peak.

The RPA calculation is far above this strength, with 100% of the strength computed for the 13.2 MeV GQR peak [11], as confirmed by a fit with the background shown in Fig. 6(b) to theory "A". This RPA calculation was also used to compute pion cross sections, using the sum of all computed strength from 9 to 19 MeV. In Ref. [11] this prediction was compared to pion data for the GQR *peak* only, and far exceed such π^+ data. This is as expected, since only about one-third of the quadrupole strength is concentrated in the coherent GQR peak.

The other path to determine the proton portion of an isoscalar GQR uses the isoscalar strength $B(02)$ from inelastic alpha-particle scattering, or from the isoscalar combination of π^- and π^+ cross sections, with the methods in Ref. [3]. These inferred $B(C2)$ strengths do not agree with those more directly obtained from electron or pion scattering, being greater by more than a factor of 2, but do agree more closely with one another, as listed in Table IV.

It is this disagreement that suggests a large and completely unexpected isovector strength at $65A^{-1/3}$ MeV, as pointed out in Ref. [11]. There is an alternative explanation, not included in the purely collective analyses, or in a model with bound oscillator wave functions, as in Ref. [11].

The isoscalar results include the neutron matrix element, which cannot be separated in alpha scattering or observed by inclusive electron scattering, but which is emphasized by π^- scattering. Positive pion scattering results dominate the determination of the proton matrix element M_p. The GQR in ^{118}Sn is unbound to both neutron and proton decay, but the Coulomb barrier effectively reduces the penetration of the proton to the continuum. If the neutron contribution to the hadronic scattering is greater than that of the proton, the "isoscalar" observables will be enhanced, and reduction by Z^2/A^2 will not return us to the proton strength. That would be true only in the collective model, which does not acknowledge binding energy effects. Scattering of such strongly absorbed projectiles as resonance pions and alphas emphasizes this process by interacting mainly in the nuclear surface [5,6,36]. Use of the collective model in this way does indeed overestimate the $B(C2)$ values. Of course, the neutron decay is central to the $(e,e'n)$ analysis, and those results also agree with the inclusive electron and π^+ data.

VI. DISCUSSION

The first systematic feature noted for the giant resonance spectrum (Fig. 3), taken with good energy resolution, is that discrete peaks end by about 10 MeV. Second, in all spectra the yield increases above the general trend of the counts just at the neutron binding energy. Since our probe interacts with only the protons of the target, any reflection of the neutron structure of the tar-

get must occur through collectivity, as pointed out by Alberico et al. [37] and used by Miskimen et al. [12]. This is presumably then due to the isoscalar collective GQR as analyzed in the present work.

For ^{118}Sn, a typical nucleus, we find much of the classical sum rule to be exhausted for the well-known GDR, seen clearly above a smooth background in our spectra, and acceptably fitted by the model of Goldhaber and Teller. This is as expected, and yields confidence in our background removal. In contrast, the GQR feature in our spectra is 0.85 MeV lower in excitation and 0.9 MeV narrower than found in alpha-particle scattering, with Gaussian peak shapes in both cases. Given the additional problems in comparing two such different experiments, these differences may not be significant. The most striking feature of our results for ^{118}Sn is the small fraction, $25\pm5\%$, of the isoscalar Coulomb sum rule exhausted for the well-determined GQR peak.

The Gaussian peak fitting and background scheme used for our analysis of peaks was selected to be consistent with that used for alpha and pion scattering on ^{118}Sn. The greater strength in alpha scattering could be due to the enhancement of the neutron contribution in the transition to the unbound final state, as suggested by model calculations including the unbound final wave functions [5]. This also could account for the observed asymmetry between π^+ and π^- scattering to the GQR [3,4,38]. One of the principal purposes of the present study was to test this concept.

The several electron-scattering measurements to the GQR of ^{118}Sn do, however, agree. The Tohuku results are derived from a multipole analysis of all counts above the elastic radiative tail [8,9]. This method finds a larger fraction of the $C2$ sum rule than does the present method, but without identification with the same coherent giant state seen in hadron scattering. Similar methods used in other inclusive analyses also result in strong $C2$ fractions [25].

Another method uses an explicit peak fitting for the giant resonances, but with the background taken to be the elastic radiative tail plus instrumental background [10]. Our background is taken to be a well-determined smooth continuum without identifying its origins. When fitted by the same methods we use, previous electron data yield 32% of the sum rule in the coherent peak.

A very recent study of GQR in ^{118}Sn by inelastic ^{17}O scattering observed a strong peak, composed of the GDR and GQR structures [39]. After subtraction of the GDR and a continuum, all the strength near 13 MeV was fitted to a Gaussian by those authors, yielding $B(C2)\!\uparrow\,=1810$ $e^2\,\mathrm{fm}^4$, or 60% of the isoscalar sum rule. When fitted by us as a Gaussian peak above a flat background as has been the practice in the present work, the strength to the coherent peak is about $830\ e^2\,\mathrm{fm}^4$, or 29% of the sum rule. This is in agreement with the other results from this process, as listed in Table IV.

Our method has been to isolate a well-determined peak above some smooth continuum, as was done in the analysis of pion scattering. Since much of the isoscalar quadrupole strength is missing from this peak, it must form part of that continuum, and has not been included

in our analysis. Since the form and content of the continuum must depend upon the scattering probe, it is difficult to compare results other than by the method we have chosen, fitting a persistent peak found in all studies.

We conclude that inelastic electron scattering to a coherent GQR peak above a smooth background at $65A^{-1/3}$ MeV in ^{118}Sn finds the same charge strength as in the same feature in pion scattering, with its much different reaction mechanism. Disagreement is found with a recent open-shell RPA calculation that locates 100% of the strength in that single peak, and the inconsistency of alpha-scattering results for inference of this strength is demonstrated.

*Present address: Institute for Nuclear and Particle Physics, University of Virginia, Charlottesville, VA 22901.

[1] A. Bohr and B. R. Mottelson, *Nuclear Structure* (Benjamin, Reading, 1975), Vol. II, pp. 507–520.

[2] D. H. Youngblood, J. M. Moss, C. M. Rozsa, J. D. Bronson, A. D. Bacher, and D. R. Brown, Phys. Rev. C **13**, 994 (1976).

[3] J. L. Ullmann et al., Phys. Rev. C **35**, 1099 (1987).

[4] S. J. Seestrom-Morris, C. L. Morris, J. M. Moss, T. A. Carey, D. Drake, J. C. Dousse, L. C. Bland, and G. S. Adams, Phys. Rev. C **33**, 1847 (1986).

[5] R. J. Peterson and J. L. Ullmann, Nucl. Phys. **A435**, 717 (1985).

[6] R. J. Peterson and R. de Haro, Nucl. Phys. **A459**, 445 (1986).

[7] R. Pitthan, F. R. Buskirk, E. B. Dally, J. O. Shannon, and W. H. Smith, Phys. Rev. C **16**, 970 (1977).

[8] S. Fukuda and Y. Torizuka, Phys. Rev. Lett. **29**, 1109 (1972).

[9] K. Hosoyama and Y. Torizuka, Phys. Rev. Lett. **35**, 199 (1975).

[10] R. Pitthan, H. Hass, D. H. Meyer, F. R. Buskirk, and J. N. Dyer, Phys. Rev. C **19**, 1251 (1979).

[11] V. R. Brown, J. A. Carr, V. A. Madsen, and F. Petrovich, Phys. Rev. C **37**, 1537 (1988).

[12] R. A. Miskimen et al., Phys. Lett. B **236**, 251 (1990).

[13] H. de Vries, C. W. de Jager, and C. de Vries, At. Data Nucl. Data Sheets **36**, 495 (1987).

[14] M. R. Braunstein, J. J. Kraushaar, R. P. Michel, J. H. Mitchell, R. J. Peterson, H. P. Blok, and H. de Vries, Phys. Rev. C **37**, 1870 (1988).

[15] J. Kelly, C. E. Hyde-Wright, and E. A. J. M. Offermann (private communication).

[16] B. L. Berman and S. C. Fultz, Rev. Mod. Phys. **47**, 713 (1975).

[17] E. F. Gordon and R. Pitthan, Nucl. Instrum. Methods **145**, 569 (1977).

[18] G. Kilgus et al., Z. Phys. A **326**, 41 (1987).

[19] G. Kühner, D. Meuer, S. Müller, A. Richter, E. Spamer, O. Titze, and W. Knüper, Phys. Lett. **104B**, 189 (1981).

[20] D. H. Youngblood, P. Bogucki, J. D. Bronson, U. Garg, Y. W. Lui, and C. M. Rozsa, Phys. Rev. C **23**, 1997 (1981).

[21] L. J. Tassie, Austr. J. Phys. **9**, 407 (1956).

[22] H. Ui and T. Tsukamoto, Prog. Theor. Phys. **51**, 1377 (1974).

[23] Program Foubes, J. Heisenberg, and H. P. Blok (unpublished).

[24] O. Nathan and S. G. Nilsson, in *Alpha- Beta- and Gamma-Ray Spectroscopy*, edited by K. Siegbahn (North-Holland, Amsterdam, 1968), Chap. X.

[25] R. Klein, Y. Kawazoe, P. Grabmayr, G. J. Wagner, J. Friedrich, and N. Voegler, Phys. Lett. **145B**, 25 (1984).

[26] M. Goldhaber and E. Teller, Phys. Rev. **74**, 1046 (1948).

[27] H. Steinwedel and M. Danos, Phys. Rev. **79**, 1019 (1950).

[28] W. D. Myers, W. J. Swiatecki, T. Kodama, L. J. El-Jaick, and E. R. Hilf, Phys. Rev. C **15**, 2032 (1977).

[29] A. Bohr and B. R. Mottelson, *Nuclear Structure* (Benjamin, Reading, 1975), pp. 399–404.

[30] T. H. Curtis, R. A. Eisenstein, D. W. Madsen, and C. K. Bockelman, Phys. Rev. **184**, 1162 (1969).

[31] R. Graetzer, S. M. Cohick, and J. X. Saladin, Phys. Rev. C **12**, 1462 (1975).

[32] F. E. Bertrand, G. R. Satchler, D. J. Horen, J. R. Wu, A. D. Bacher, G. T. Emery, W. P. Jones, D. W. Miller, and A. van der Woude, Phys. Rev. C **22**, 1832 (1980).

[33] C. M. Rozsa, D. H. Youngblood, J. D. Bronson, Y. W. Lui, and U. Garg, Phys. Rev. C **21**, 1252 (1980).

[34] J. L. Ullmann et al., Phys. Rev. C **31**, 177 (1985).

[35] G. Duhamel, M. Buenerd, P. de Saintignon, J. Chauvin, D. Lebrun, P. Martin, and G. Perrin, Phys. Rev. C **38**, 2509 (1988).

[36] P. M. Boucher and B. Castel, Z. Phys. A **334**, 381 (1989).

[37] W. M. Alberico, G. Chanfray, M. Ericson, and A. Molinari, Nucl. Phys. **A475**, 233 (1987).

[38] D. S. Oakley, M. R. Braunstein, J. J. Kraushaar, R. A. Loveman, R. J. Peterson, D. J. Rilett, and R. L. Boudrie, Phys. Rev. C **40**, 859 (1989).

[39] D. J. Horen, F. E. Bertrand, J. R. Beene, G. R. Satchler, W. Mittig, A. C. C. Villari, Y. Schutz, Z. Wenlong, E. Plagnol, and M. Matsuzaki, Phys. Rev. C **42**, 2412 (1990).